Original Paper

Eletrônica de Potência
Open Journal of Power Electronics

Received July 08, 2024; accepted November 27, 2024; Date of publication January 14, 2025.
The review of this paper was arranged by Associate Editor Fernanda de M. Carnielutti and Editor-in-Chief Telles B. Lazzarin.

Digital Object Identifier http://doi.org/10.18618/REP.e202504

Methodology for Fault Detection Applied in Photovoltaic Plants Based on Inverter Power Curve Analysis

Paulo A. V. Vieira[1], **João M. S. Callegari**[2], **Heverton A. Pereira**[1]

[1]Federal University of Viçosa, Dept. of Electrical Engineering, Viçosa, MG, Brazil
[2]Federal University of Minas Gerais, Dept. of Electrical Engineering, Belo Horizonte, MG, Brazil

e-mail: paulo.alberto@ufv.br, jmscallegari@ufmg.br, heverton.pereira@ufv.br

ABSTRACT The maintenance of photovoltaic plants is crucial to ensure their proper performance, longevity, and efficiency, while also enhancing the return on investment and contributing to sustainable energy production. In such context, this paper proposes a methodology to characterize the main issues in photovoltaic plants, based on the analysis of the proposed inverter output power curve. Through power curve analysis, the most common anomalies and faults encountered in inverters are identified, providing a valuable tool for the early detection of operational issues. Additionally, power curve analysis allows a comparison between projected and actual values of generated energy, offering an index of system energy losses. Lastly, an economic analysis is presented, ranking inverters based on the magnitude of their energy losses, from highest to lowest. This analysis provides important insights for prioritizing maintenance actions and allocating resources to enhance generation returns.

KEYWORDS Photovoltaic inverters, irradiance, power, energy loss, fault detection.

I. INTRODUCTION

Rising interest in renewable energy has led to the globally widespread expansion of photovoltaic (PV) solar power plants [1]. This ongoing PV growth is essential for achieving global sustainability goals and reducing greenhouse gas emissions [2]. The PV industry has become increasingly consolidated and mature worldwide, marked by the commercialization and installation of relatively affordable large-scale PV systems in recent decades [3]. As more PV systems are deployed, ensuring their efficiency and longevity becomes crucial, generating a growing demand for specialized maintenance services [4]. Operation and maintenance (O&M) of PV systems are increasingly seen as crucial to ensuring their proper long-term performance and, consequently, achieving expected financial returns [5], [6]. The lack of an appropriate schedule of maintenance affects the power generation performance and can also decrease the PV system's lifetime [7].

Large-scale PV plants require significantly more attention regarding O&M and monitoring systems compared to small-scale rooftop PV systems since corrective maintenance can result in prolonged downtime and substantial financial losses. These PV systems consist of tens to hundreds of thousands of PV modules mounted on ground structures, often equipped with single- or double-axis solar trackers [8]. The PV plants are connected to the medium and high voltage upstream grid through PV skids embedded with step-down transformers [9]. PV skids receive AC-side cables from the inverters to switchgears, providing AC protection through properly coordinated and selective circuit breakers. String or combiner boxes are employed for interconnection and protection of PV modules, including fuses, circuit breakers, surge protectors, and grounding systems to protect the DC-side PV system from electrical faults and lightning strikes. Meteorological stations are deployed to measure environmental variables, including solar irradiance, temperature, and wind speed, all of which significantly influence the performance of the PV system [10]. Additionally, monitoring systems are implemented to ensure real-time recording of PV power plant parameters [11]. A supervisory control and data acquisition (SCADA) system can integrate all inverters into a single interface while also receiving external commands from the distribution grid operator [12]. All of this equipment represents a potential point of failure or point of reduced efficiency, requiring maintenance in case of improper operation [13].

Advancements in technology have allowed the inspection and failure diagnosis of PV systems, enabling non-destructive and non-contact diagnostic methods. The dataset acquired by monitoring systems is crucial for the O&M team to conclude on the PV plant performance and propose predictive and preventive maintenance strategies. For instance, the authors of [13] developed a failure rate analysis based on an extensive field-derived dataset sampled from different large-scale PV systems over three to five years. Reference [14] compared and discussed the performance ratios obtained from 235 PV installations in Germany and 133 PV plants in other countries. A statistical approach for estimating energy losses resulting from the deposition of soiling on PV module is addressed in [7]. The authors of [15] address aerial thermography as a useful diagnostic technique for the inspection of PV plants. This approach supersedes

time-consuming traditional manual methods, offering a more efficient means of evaluating PV systems. Villarini et al. [16] collected failure and maintenance-related data to revise the maintenance strategy of the PV systems and to optimize their efficiency. Reference [17] shows a fault prediction solution tested on six PV plants, each up to 10 MW, and over one hundred invertes. The authors found the method capable of effectively predicting incipient generic faults up to 7 days in advance with sensitivity up to 95%; and anticipating damage of specific fault classes with times ranging from a few hours up to 7 days. As noted, a major part of the existing literature focuses on the maintenance assessment of specific components, such as the inverter [18], or PV module's individual elements [19].

Further exploration and a straightforward step-by-step procedure are required to effectively monitor the performance of PV systems. This paper proposes a methodology based on the inverter power curve (IPC) to identify possible field issues based on the behavior of experimental data. According to the literature [20] [21] [22] power curve modeling techniques have been broadly applied in wind turbines for identifying failure profiles, energy estimation, and energy forecasting. An up-to-date dataset of large-scale field PV plants is applied to the proposed methodology, which identifies and highlights equipment that should be analyzed by the O&M team for maintenance purposes. Thus, the O&M team can accurately classify losses for each component and take decisive actions to identify faults and pinpoint where the greatest revenue loss is occurring. Performance analysis of inverters in large PV plants is also conducted to identify trends of failure and potential causes of inefficiency. The findings of this paper hold great value for investors in PV-based renewable energy since this proposal facilitates prompt decision-making to identify and resolve prolonged inefficiencies resulting from generation shortfalls.

This work comprises five Sections. This section provides an overview of the national scenario regarding photovoltaic generation plants and outlines the objectives and contributions of this paper. Section II discusses the development of the proposed inverter power curve in detail. Section III addresses the methodology for calculating energy loss using the proposed inverter power curves. Section IV identifies potential inverter-level issues. In Section V, the case study was introduced and the real-field results of inverter power curves for each type of inefficiency in a specific photovoltaic power plant (PVPP) were presented. Finally, the conclusions are stated in Section VI.

II. INVERTER POWER CURVE

Once operational, the real-field PVPP generation must be compared with the projections presented in the Solar Resource Energy Assessment (SREA) to verify alignment between expected and actual generation. The expected generation can be obtained using well-established software available on the market, such as PVsyst [23] and PV*Sol [24]. An alternative to verify the alignment between actual and expected generation is through IPC.

The IPC modeling is defined as a mathematical model that describes the inverter output power (i.e., P_{ac}) as a function of the irradiance measured by front and rear pyranometers. The former pyranometer measures the global tilted irradiance (GTI), while the latter measures the global rear irradiance (GRI). This modeling allows for a comparison between actual and projected production, enabling the identification of any deviations or generation losses of the inverters.

The IEC 61724 standard (1, 2, and 3) provides globally recognized and accepted guidelines for evaluating PV generation system performance [25]. While this work references the standard as a foundation framework, it does not rely solely on it. Specific aspects of the standard, such as data sampling rates and sensor maintenance, are adopted to align with industry practices. However, the analyses and methodologies introduced in Sections II and III extend beyond the standard's scope, offering original contributions to the field of fault detection in PV plants.

A. Historical power curve

The historical power curve serves as a reference for estimating the projected production or potential yield of the specific system. It indicates how much energy the inverter should produce according to predefined design conditions and based on historical solar irradiance data from the area where the system is installed. Through simulation using specialized software, it is possible to determine the expected output power of the inverter based on the solar irradiance values. This allows to establish a relationship between the inverter output power (P_{ac}) and irradiance (Irr). This methodology produces a standard curve based on statistical analyses, which represents the relationship between output power and irradiance and serves as a tool for fault and inefficiencies detection. In addition, this curve can be used to estimate the inverter energy losses. Figure 1 shows an example of a historical curve for an inverter, illustrating how the output power varies with irradiance over time. For easy reference, all irradiance variables are defined in Figure 1. The IPC shown in Figure 1 can be categorized into three regions:

- **Region 1:** No generation or inverter start-up region ($Irr < Irr_{start}$). In this region, the inverter starts up based on the minimum irradiance necessary to generate current and voltage in the photovoltaic modules.
- **Region 2:** Inverter power ramping up/down region ($Irr_{start} \leq Irr \leq Irr_{clipping}$). Region 2 comprises the operation of the inverter throughout the day.
- **Region 3:** Power clipping region (Irr $\leq Irr_{\text{clipping}} \leq Irr_{\text{max,clipping}}$). In region 3, the inverter operates at its rated capacity, entering into the power clipping region.

The historical power curve is applied for analysis of an inverter at the power converter system (PCS) level. However,

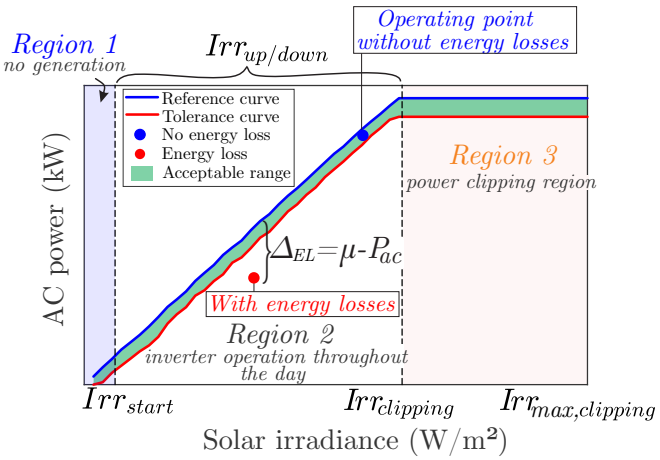

FIGURE 1: Generic inverter historical power curve.

such analysis can be extended to various PVPP topologies, as follows:

- String inverter: one historical power curve for each string inverter;
- Central inverter: one historical power curve for each central inverter;
- Virtual central inverter: one historical power curve for each inverter.

For string inverters, a practical approach is to develop a power curve based on the combined outputs of all inverters connected to the respective PCS, given the high number of inverters typically installed in a project. However, it is noteworthy that this simplification may limit the ability to identify potential issues in individual inverters.

B. Construction of the reference power curve

The period for constructing the IPC should be at least one year to account for all seasonal variations when the SREA is not available. Additionally, the latest version of the SREA should always be used for constructing the power curve, as it ensures the use of the most up-to-date and accurate data. The steps for the construction of the reference power curve are summarized as follows:

1) Obtain the hourly file from a specialized PV-based simulation software containing the following variables:
   - Output AC power of the inverter [kW];
   - Global tilted irradiance - GTI [W/m^2];
   - Global rear irradiance - GRI [W/m^2];
   - PV module temperature [°C];
   - All data should have the same timestamp.
2) Filter out anomalous data from the database (outliers), if applicable.
3) Separate the solar irradiance values into intervals of 30 W/m^2, which will be referred to as irradiance bins. These bins are arranged in a histogram, where the mean power value (μ) of each bin is calculated to form a point on the reference curve shown in Figure 1.
4) After completing the construction of the reference curve, the tolerance curve is done through the margin of error, essentially a measure of uncertainty in the obtained extrapolation, which can be calculated by [26]:

$$\lambda = \mu - 2.5\sigma, \tag{1}$$

with:

$$\sigma = \sqrt{\sum_{j=1}^{J}(X_n(j) - \mu)^2}, \tag{2}$$

where σ corresponds to the standard deviation of the distribution of power values associated with each irradiance bin. λ is the lower tolerance power curve, considering 2.5 standard deviations. The final IPC with the upper (reference) and lower (tolerance) limits is presented in Figure 1.

C. Correction of solar irradiance based on temperature

As previously addressed, the reference curve is developed using historical SREA data. To accurately obtain real-field values, solar irradiance is corrected as a function of temperature, as PV modules lose efficiency with temperature increase. Thus, the temperature correction factor is applied when the PV module temperature measured is above the standard test conditions (STC) [27]:

$$k = 1 + \gamma(T_{\text{mod}} - T_{\text{mod(STC)}}), \tag{3}$$

where k is the module temperature correction constant, γ is the module temperature coefficient, T_{mod} is the actual module temperature measured by PT100 sensor (°C), and $T_{\text{mod(STC)}}$ is the module temperature at STC (i.e., 25 °C). Finally, the irradiance is corrected for temperature using the following equation:

$$Irr_{corr} = k \cdot Irr_{total}, \tag{4}$$

where Irr_{corr} corresponds to the measured real-field irradiance value in [W/m^2]. Currently, many PV plants have employed bifacial technology modules, thus, the Irr_{total} value will change due to the gain in bifaciality, defined by the expression:

$$Irr_{total} = Irr_{GTI} + Irr_{GRI} \cdot FB, \tag{5}$$

where Irr_{GTI} corresponds to the irradiance value on the module surface [W/m^2], Irr_{GRI} is the irradiance on the back of the panel [W/m^2], and FB is the module bifaciality factor.

III. ANALYSES THROUGH THE POWER CURVE

In this section, a methodology for calculating energy losses (EL) per inverter using the IPC will be presented. Additionally, the main issues encountered in PVPPs will be explored.

A. Calculation of energy losses

For each inverter, the associated EL is determined by summing the individual deviations at each point plotted on the IPC. As observed in Figure 1, this can be summarized into two scenarios:

1) **No energy loss**: In this scenario, the j-th power point fall within the reference and tolerance limits of the power curve. Thus:

$$\lambda \leq P_{\text{ca}}(j) \leq \mu. \tag{6}$$

2) **Energy loss**: In this scenario,the j-th power point is below the tolerance curve. Thus:

$$P_{\text{ca}}(j) < \lambda. \tag{7}$$

Finally, to obtain the consolidated j-th energy loss (i.e., $\Delta_{EL}(j)$), the following expression is applied:

$$\Delta_{EL}(j) = \begin{cases} 0, & \text{if} \quad \lambda \leq P_{ac}(j) \leq \mu \\ \lambda - P_{ac}(j), & \text{if} \quad P_{ac}(j) < \lambda \\ 0, & \text{if} \quad P_{ac}(j) > \mu, \end{cases} \tag{8}$$

where the j-th energy loss is non null only when $P_{ac}(j) < \lambda$. The total EL (i.e., EL_{total}) is determined by:

$$EL_{total} = \sum_{j=1}^{J} \Delta_{EL}(j), \tag{9}$$

where J represents the total number of points in the evaluated database.

B. Energy loss index

Once the EL value is obtained, normalization is carried out using the energy loss index (ELI). This indicator is expressed by:

$$ELI = \frac{EL_{total}}{EL_{PZ}}, \tag{10}$$

where EL_{total} corresponds to the energy loss for the period under analysis calculated in (9), and EL_{EZ} is the expected energy production, i.e., the amount of energy that was expected to be generated at the same period. Thus, EL_{PZ} has the following values:

$$EL_{PZ} = \begin{cases} \sum_{j=1}^{J} P_{ca}(j), & \text{if } P_{ca}(j) > \lambda \\ \sum_{j=1}^{J} \mu(j), & \text{if } P_{ca}(j) \leq \lambda \end{cases} \tag{11}$$

According to the definition in (11), when the power value is within or above the established limits, the measured power value is used. Conversely, if the power point is below the tolerance curve, the reference curve value is used. Thus, ELI serves as a guidance tool for the O&M team, providing insights into which equipment is experiencing higher energy losses. This enables the O&M team to improve their interventions by prioritizing underperforming equipment, to increase system efficiency.

IV. IDENTIFICATION OF FAULTS THROUGH CURVE PROFILES

The difficulty of PVPP monitoring, in terms of parameters and precision, depends on its complexity and size. An important factor is the sampling rate at which the data is stored. IEC 61724 standard specifies that data should be recorded at least every 5 minutes [25]. With the collected data, the power values of the inverters and the corrected total irradiance (Irr_{tot}) are plotted. However, the system is susceptible to data losses, which are usually stored on the local server and often retrieved through the buffer. The obtained data are plotted daily on an accumulative basis. Some alternatives are presented in case of missing data:

- Inverter without communication: Local data extraction (inverter) and subsequent upload to the server.
- Irradiance (Irr): Local extraction (datalogger) of data and subsequent upload to the server. If the plant has more than one sensor, use data from the nearest sensor or the average of sensors. If no sensors are available, use satellite data. If the pyranometer used is installed on a tracker with a defect (stopped), repair the tracker. Otherwise, choose another sensor as a reference.
- Panel temperature: Local extraction (datalogger) of data and subsequent upload to the server. If the plant has more than one sensor, use data from the nearest sensor or the average of sensors.

The raw data collected must be processed to eliminate outliers, negative or very high values, and frozen data. The IPC allows for the quick detection and detailed analysis of potential losses in inverter generation by identifying fault patterns in its curve profile.

A. String box or PV string out of operation

Through the IPC, it is possible to identify if the inverter has one or more string boxes (SBs) out of operation. In this case, the curve will tend to stay consistently below the tolerance curve across the entire range of irradiance values, and the inverter cannot reach its rated power. Figure 2(a) shows this curve profile.

B. DC failure

In this case, unlike the previous scenario, the IPC tends to stay below the tolerance curve for medium to high irradiance values (i.e., Irr higher than 500 W/m^2), and the inverter cannot reach its rated power. Identifying this curve profile, as shown in Figure 2(b), indicates that the inverter is operating with a DC value below expectation. Possible causes of inefficiency could include a string fuse that has burned out or PV modules that have been damaged.

C. Soilling

PV plants employ sensors to monitor soiling to determine the proper time for module cleaning. However, the number of installed sensors often does not accurately reflect the

condition of the entire PV plant. To assist in verifying this information, IPC can be employed. In such cases, the curve will display a profile consistently below the lower limit throughout the generation period, with a similar pattern observed in other inverters. Figure 2(c) illustrates the curve affected by soiling.

D. Tracker in 0° position

This type of inefficiency occurs when the tracker is in 0° position, meaning it remains completely in horizontal position throughout the day. In this scenario, the curve will exhibit a parabolic shape below the tolerance curve, indicating an inefficiency, as shown in Figure 2(d). Thus, with the sun rising in the east and increasing irradiance throughout the day, the power generated by the inverter will not follow the MPPT. Only during the period near noon, when the tracker is at 0°, will the curve fall within the limits. The same behavior is observed after noon, as irradiance decreases with the sun setting in the west.

E. Tracker with misalignment failure ($\theta_{real} \neq \theta_{tgt}$)

In this case, the tracker angle θ_{real} differs from the target angle θ_{tgt} at some point during the day. Although the tracker is operational, this discrepancy is causing inefficiency. Therefore, the O&M team should check the configured setpoint and/or conduct a field inspection to identify any issues. The curve is shown in Figure 2(e), where several points form a smaller parabola on the x-axis. This issue could be identified either in the morning or the afternoon.

F. Tracker with pyranometer at 0°

In this scenario, the tracker equipped with pyranometers GTI and GRI (if applied) is positioned at 0°, remaining completely horizontal throughout the day. In this configuration, the curve will exhibit a parabolic shape, similar to that shown in Figure 2(d). However, the curve will be situated above the reference curve, as depicted in Figure 2(f). Consequently, the inverter power will increase throughout the day, while the measured irradiance will be lower at higher inverter power levels. Only around noon, when the tracker is at 0°, will the curve fall within the acceptable limits. Additionally, any energy loss will be misestimated in this scenario, as all points will be above the reference curve, leading to an incorrect estimation of energy loss.

G. Inverter with power derating

In the event of a possible derating (i.e., a reduction in the inverter's power output due to an increase in internal or external temperature), the points on the power curve tend to cluster and remain below the lower curve for irradiance values above 700 to 800 W/m°. This clustering of points does not occur at low irradiance values. Figure 2(g) illustrates the scenario of the inverter experiencing derating.

H. Inverter out of operation

When the inverter is out of operation, the points will lie on the x-axis, as the power output remains zero even as the irradiance increases throughout the day. This failure profile is depicted in Figure 2(h).

I. Power limitation

This case is shown in Figure 2(i). It is possible to observe a horizontal power line on the x-axis, varying according to the irradiance value at the moment. Additionally, this type of scenario occurs for several inverters in the PV plant. This analysis can also be extended to identify any power limitation in the inverter.

J. Sensors not working correctly

In addition to the aforementioned failures, an important point concerns the sensors (i.e., pyranometers and PT100 sensors). When these sensors malfunction, the measured power curve profile will be altered, resulting in erroneous EL values. The most common situations are:

- Dirty pyranometer;
- Uncalibrated pyranometer;
- Misaligned pyranometer concerning the tracker;
- Shaded pyranometer;
- PT100 peeling off or detached from the module;
- PT100 fixed in the wrong place (trace);
- Tracker with the sensors stopped;

For example, the plotted values tend to be above the reference curve for a dirty pyranometer, as shown in Figure 2(j). In this scenario, the points will be displaced above the reference curve, which could, in some cases, mislead the system energy losses and key performance indicator (KPI) calculations. Figure 2(k) shows a curve where the PT100 sensor is displaced from the panel, measuring the ambient temperature instead. In this case, the points tend to be displaced to the right, resulting in an erroneous deviation from the expected energy. Additionally, if the points fall below the tolerance curve, the EL will increase.

K. Communication failure

Finally, there is a scenario where communication is lost due to intermittent data losses. In this case, the curve will show only a few plotted points, as depicted in Figure 2(l). Additionally, it is possible to identify some points on the y-axis, indicating that only inverter data is available.

V. CASE STUDY

In this section, a case study will be conducted using the IPC for a PV plant located in the southwest region of Brazil. The PV plant is composed of 14 string inverters, separated into two generation units (GU), with a total installed capacity of 3.6 MWp. Each GU is designated as A or B and comprises 7 inverters. In GU-A, the inverters are named from $1A1$ to

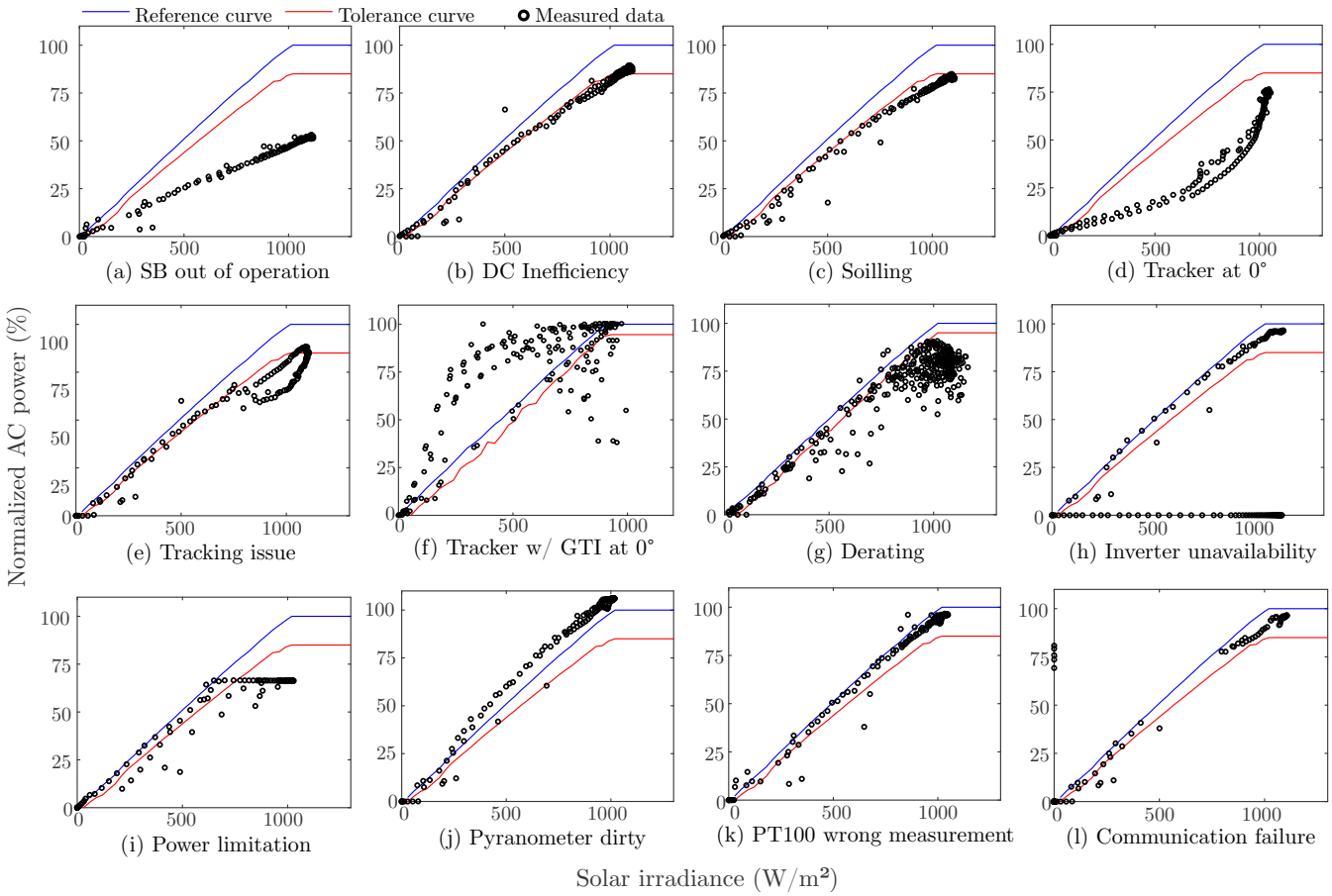

FIGURE 2: Failures and anomalies identified through inverter power curve profiles: (a) SB or PV string out of operation; (b) DC inefficiency; (c) soiling on the PV modules; (d) tracker in 0° position; (e) tracker with misalignment failure; (f) tracker with pyranometer at 0°; (g) inverter with power derating; (h) inverter out of operation; (i) power limitation; (j) sensors not working properly; and (k) communication failure.

$1A7$, while in GU-B, the inverters are named from $1B1$ to $1B7$. Below are the premises adopted for the analysis:

- The analyzed data corresponds to one week. Although the IPC is constructed using one year of data, analyzing a reduced data set over a one-week period facilitates clearer visualization and a more focused understanding of the described phenomena;
- Power, solar irradiance, and module temperature data were collected every five minutes through the PV plant's SCADA;
- The generated reference curve was developed with the as-built version of the SREA, post-performance testing;
- The kWh price was considered as R$ 0.59599.

The simplified schematic diagram of the PVPP used in this work is shown in Figure 3. The analysis are based on a one-week dataset for clarity, however analyses can also be conducted on a daily or monthly basis depending on specific needs. For instance, a monthly summary of losses might be sufficient for company management, whereas weekly data could be more practical for the O&M team to plan and execute necessary interventions. With a robust system and dedicated team, daily analyses could be feasible. Ultimately, the choice of analysis frequency depends on the resources available to the O&M team. In summary, the fault characterization is supported by extensive data covering any time basis or period considered (e.g., over a year).

A. Inverter analysis

As presented in Section II, the analysis of the inverter power curve reveals crucial information about potential energy losses. The IPC and real-field one-week data for AC power and solar irradiance are presented in Figure 4 for several inverters in the PVPP. For inverter 1A6, Figures 4(a.1)-(a.3) demonstrate normal operation, as evidenced by the continuous data points remaining within the boundary limits of the IPC.

In Figures 4(b.1)-(b.3), the inverter exhibited a power limitation over several days. This is evidenced by the concentration of points close to 75% of the inverter's rated capacity. This analysis enables a more accurate certification

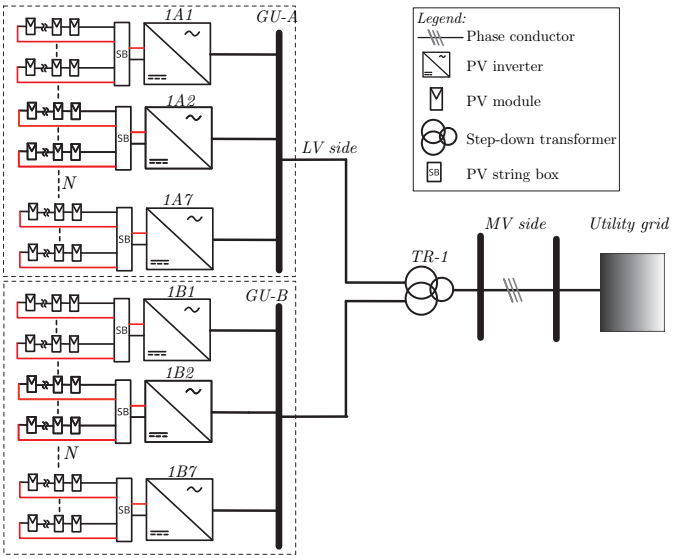

FIGURE 3: Simplified single-line diagram of the PV plant employed in the case study.

of the power limitation during this period. Additionally, it is observed that the inverter underwent corrective maintenance to address the power limitation issue. This resulted in points on the x-axis, where $P_{ac} = 0$ W and Irr higher than $800\,\mathrm{W/m^2}$.

The inverter shown in Figure 4(c.1)-(c.3) exhibits behavior indicative of a PV tracker problem. The day begins with the tracker at an angle of 0°, and it returns to its normal pattern around noon. However, on the following day, the tracker did not initiate its operation, remaining at 0° throughout the day, as reflected in the presented curve profile. After the tracker was repaired, the inverter returned to its normal operating pattern. However, it remains necessary to repair the strings to fully restore the inverter to its optimal operating condition.

The inverter 1B5, shown in Figures 4(d.1)-(d.3), was out of operation for one day, as indicated by the points located on the x-axis. Other inverters did not exhibit any critical behavior indicative of significant failures. However, the analysis revealed some irregularities in the tracking system, warranting a more detailed on-site investigation by the O&M team. For instance, Figures 4(e.1)-(e.3) illustrate the performance of inverter 1B4, which also requires closer examination. This investigation is essential for identifying and resolving any potential issues that may impact the efficiency and reliability of the PVPP.

Table 1 presents the analyzed values for GU-A sector over the study period. It is observed that some inverters are operating below their maximum production capacity, as indicated by the relative error (i.e., comparison between the highest-producing inverter, 1A3, and the others in the same GU). The EL and ELI provide a measure of the deviation between the potential generation and the actual real-field production.

The inverter 1A4 exhibits the highest values for both EL at 1292.89 kWh and ELI at 10.27% for GU-A, indicating a significant power limitation, as evidenced in Figure 4(b.1)-(b.3). In contrast, the inverter 1A6 presented the lowest EL at 20.99 kWh and a correspondingly lower ELI at 0.17%. These indicators provide clear guidance for the O&M on which equipment is experiencing the greatest energy losses. This enables the O&M team to act decisively to identify and perform troubleshooting on the main cause of the power limitation, thereby contributing to the recovery and return to operation of the affected equipment. This proactive approach is crucial for enhancing the overall performance of the photovoltaic plant and increasing energy generation.

Table 2 presents the performance metrics for GU-B inverters.

In this instance, inverter 1B5 exhibited the highest EL of 1875.9 kWh and ELI of 14.99%, primarily due to one day of non-operation. Additionally, inverter 1B2 is identified as experiencing tracker issues, which likely contributed to its performance problems. It can also be inferred that this inverter had at least one string out of operation, given that it reached a maximum power value of only 86% during the period. Similarly, inverter 1B4 recorded a significant energy loss of 299.94 kWh and an ELI of 2.54%. By aggregating the values presented in Tables 1 and 2, the total EL for the period amounts to 5,393.88 kWh, resulting in a total ELI of 3.1%.

These results highlight the importance of a detailed analysis of inverter performance to identify and correct operational issues that may negatively affect energy generation at the PVPP. However, conducting preventive and predictive maintenance becomes mandatory to avoid high inefficiency indicators at the PV plant.

B. Financial loss

To analyze the financial effect of energy loss over one week for each inverter, Table 3 presents the revenue loss in R$ per kWh (i.e., R$/kWh). The values are listed for each inverter in descending order, from the highest revenue loss to the lowest.

As observed, inverter 1B5 exhibits the highest revenue loss due to an inverter failure, followed by inverter 1A4, which experienced a power limitation. According to the O&M field register, the failure of inverter 1B5 is attributed to an outage caused by a blown AC fuse, while the power limitation in inverter 1A4 resulted from an internal fan problem. The replacement costs for all these malfunctions are considerably lower compared to the financial losses resulting from the inverters' operational inefficiency.

Another crucial point to consider is the operational expenditure (OPEX) involved in the project, especially since many inverters are located in different geographical regions. Each region has its own maintenance team responsible for multiple plants in distant cities, adding complexity and cost to the maintenance operations. In this context, it becomes essential

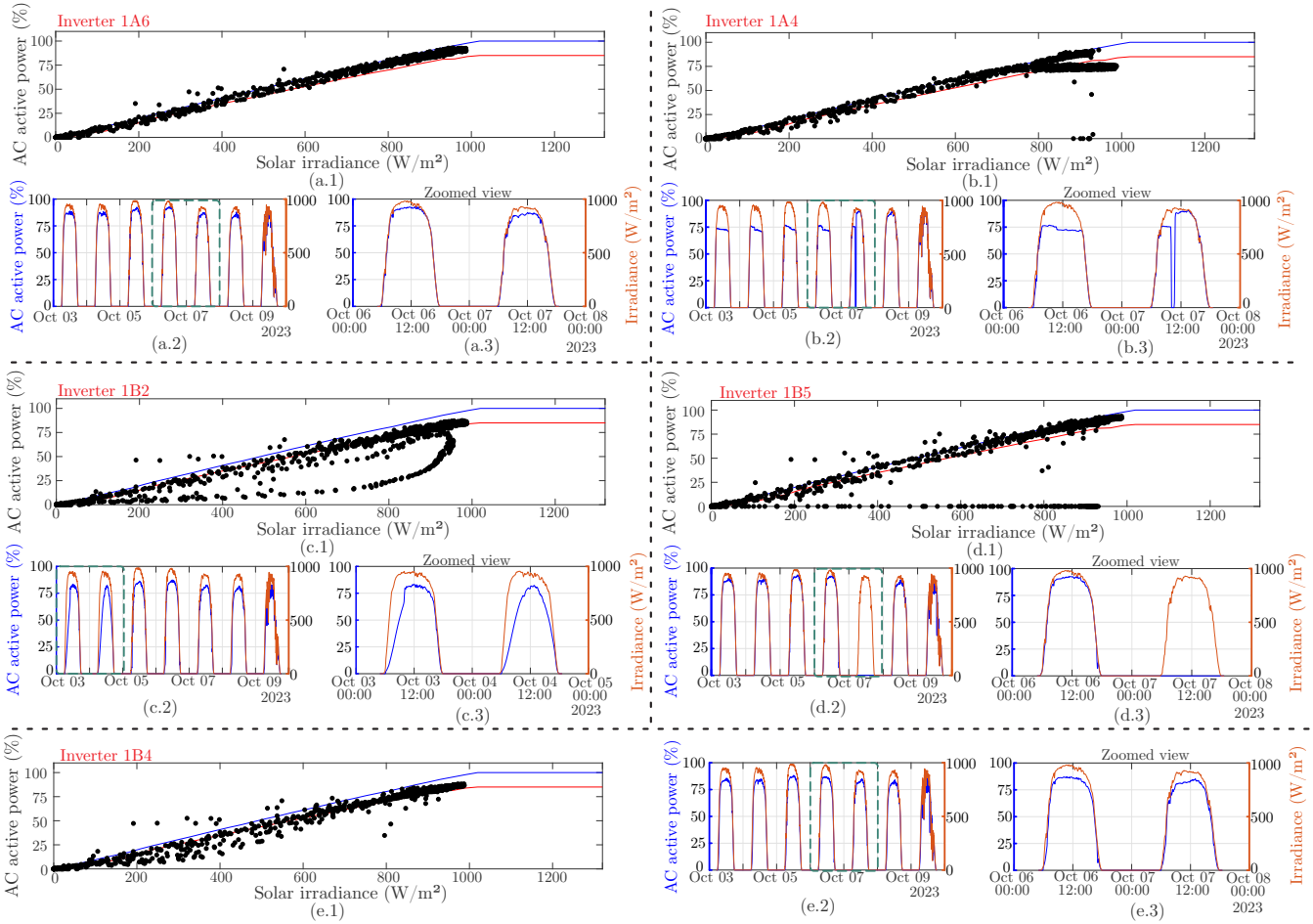

FIGURE 4: IPC for: (a.1) inverter 1A6; (b.1) inverter 1A4; (c.1) inverter 1B2; (d.1) inverter 1B5; and (e.1) inverter 1B4. One-week data of AC power and solar irradiance for: (a.2) inverter 1A6; (b.2) inverter 1A4; (c.2) inverter 1B2; (d.2) inverter 1B5; and (e.2) inverter 1B4. Two-day zoomed view of AC power and radiance data for: (a.3) inverter 1A6; (b.3) inverter 1A4; (c.3) inverter 1B2; (d.3) inverter 1B5; and (e.3) inverter 1B4.

TABLE 1: Performance metrics for GU-A inverters.

Inverter	**1A1**	**1A2**	**1A3**	**1A4**	**1A5**	**1A6**	**1A7**
Production (kWh)	12115.88	12281.84	12438.07	11299.31	12226.93	12282.46	12119.46
Expected Generation (kWh)	12247.68	12382.71	12520.29	12592.20	12294.26	12303.44	12146.46
Error (%)	-2.6%	-1.3%	0.0%	-9.2%	-1.7%	-1.3%	-2.6%
Energy loss (kWh)	131.80	100.87	82.22	1292.89	67.32	20.99	27.00
Energy loss index (%)	1.08%	0.81%	0.66%	10.27%	0.55%	0.17%	0.22%

to conduct a detailed financial analysis to determine whether it is more advantageous to immediately deploy the team to perform the repair or to wait for an opportune moment when travel costs and associated expenses are lower than the revenue loss resulting from the inefficiency. Therefore, the decision to act immediately or wait for a more favorable opportunity should consider not only financial aspects but also operational and logistical factors to ensure the long-term efficiency and profitability of the system.

Additionally, the same analysis can be applied to utility-scale photovoltaic plants. However, utility-scale plants have a higher number of equipment to manage and a dedicated O&M staff who can address identified issues more quickly. Consequently, this increases plant availability and performance, as most O&M contracts are based on these KPIs.

VI. CONCLUSION

In this work, the IPC was proposed as a tool to simplify the calculation of losses and analysis of inefficiencies in

TABLE 2: Performance metrics for GU-B inverters.

Inverter	1B1	1B2	1B3	1B4	1B5	1B6	1B7
Production (kWh)	12648.48	10629.98	12300.62	11519.20	10640.45	12605.27	12457.22
Expected Generation (kWh)	12727.54	11795.31	12407.70	11819.14	12516.34	12668.07	12537.90
Error (%)	0.0%	-16.0%	-2.8%	-8.9%	-15.9%	-0.3%	-1.5%
Energy loss (kWh)	79.06	1165.33	107.08	299.94	1875.90	62.80	80.68
Energy loss index (%)	0.62%	9.88%	0.86%	2.54%	14.99%	0.50%	0.64%

TABLE 3: Lost revenue for all inverters

Inverter	Energy loss (kWh)	Lost Revenue (R$)
1B5	1875.8971	1,118.02
1A4	1292.8856	770.55
1B2	1165.3347	694.53
1B4	299.9410	178.76
1A1	131.8045	78.55
1B3	107.0816	63.82
1A2	100.8692	60.12
1A3	82.2245	49.00
1B7	80.6778	48.08
1B1	79.0595	47.12
1A5	67.3238	40.12
1B6	62.7992	37.43
1A7	26.9976	16.09
1A6	20.9863	12.51
Total	**5393.8823**	**3,214.70**

photovoltaic plant inverters. The cases were based on real-field data from the photovoltaic plant datalogger. As a result, it was possible to identify specific fault patterns reflected in the curve profiles through the IPC analysis, which serving as indicators that something may be outside the expected standard of the inverters. Based on this information, the O&M team can make more assertive decisions and even prevent more serious problems before they occur. The analysis of the IPC offers a detailed view of the operational performance of the inverters, allowing for more efficient and proactive management of the plant's assets.

The proposed IPC approach effectively detected operational anomalies in the photovoltaic plant, although it was limited in identifying their exact causes. For future research, adopting advanced identification algorithms to improve the accuracy, reliability, and practicality of simultaneous multi-curve analysis is strongly recommended. Neural networks, in particular, offer significant promise due to their ability to learn and recognize complex patterns in extensive datasets. Unlike traditional methods, neural networks can model non-linear relationships and adapt to evolving data, making them a valuable tool for detecting faults that may be missed by conventional statistical approaches. Other promising algorithms for future exploration include support vector machines, random forests, and decision trees. Incorporating these advanced methods could greatly enhance fault detection capabilities with IPC, leading to improved reliability and operational PV plant efficiency.

In conclusion, fault detection depends significantly on the precision, availability, and quality of power, solar irradiance, and temperature data, along with the accuracy of simulations predicting the system's expected behavior. Additionally, investment in system monitoring corresponds to the importance of detecting losses and anticipating O&M equipment intervention, which ultimately impacts final energy generation and company revenue.

ACKNOWLEDGMENT

The authors are grateful for the financial support provided by CNPq (Conselho Nacional de Desenvolvimento Científico e Tecnológico) – project 407926/2023-2 and FAPEMIG (Fundação de Amparo à Pesquisa do Estado de Minas Gerais) – projects APQ-02805-23 and APQ-03164-24.

AUTHOR'S CONTRIBUTIONS

P. P. V. VIEIRA: Conceptualization, Data Curation, Formal Analysis, Funding Acquisition, Investigation, Methodology, Project Administration, Resources, Software, Validation, Visualization, Writing – Original Draft, Writing – Review & Editing. **J. M. S. CALLEGARI**: Formal Analysis, Investigation, Methodology, Supervision, Validation, Visualization, Writing – Original Draft, Writing – Review & Editing. **H. A. PEREIRA**: Conceptualization, Formal Analysis, Investigation, Methodology, Project Administration, Resources, Supervision, Validation, Visualization, Writing – Original Draft, Writing – Review & Editing.

PLAGIARISM POLICY

This article was submitted to the similarity system provided by Crossref and powered by iThenticate – Similarity Check.

REFERENCES

[1] L. S. Paraschiv, S. Paraschiv, "Contribution of renewable energy (hydro, wind, solar and biomass) to decarbonization and transformation of the electricity generation sector for sustainable development", *Energy Reports*, vol. 9, pp. 535–544, 2023, doi:https://doi.org/10.1016/j.egyr.2023.07.024, technologies and Materials for Renewable Energy, Environment and Sustainability.

[2] P. Choudhary, R. K. Srivastava, "Sustainability perspectives- a review for solar photovoltaic trends and growth opportunities", *Journal of Cleaner Production*, vol. 227, pp. 589–612, 2019, doi:https://doi.org/10.1016/j.jclepro.2019.04.107.

[3] A. Aleksandra, B. P. Sara, J. Małgorzata, B. Brian, P. Davide, C. Miguel, "Role of solar PV in net-zero growth: An analysis of international manufacturers and policies", *Progress*

in Photovoltaics: Research and Applications, vol. n/a, no. n/a, doi:https://doi.org/10.1002/pip.3797.

[4] A. Baklouti, L. Mifdal, S. Dellagi, A. Chelbi, "An Optimal Preventive Maintenance Policy for a Solar Photovoltaic System", *Sustainability*, vol. 12, no. 10, 2020, doi:10.3390/su12104266.

[5] K. Keisang, T. Bader, R. Samikannu, "Review of Operation and Maintenance Methodologies for Solar Photovoltaic Microgrids", *Frontiers in Energy Research*, vol. 9, 2021, doi:10.3389/fenrg.2021.730230.

[6] R. C. de Barros, W. C. S. Amorim, W. d. C. Boaventura, A. F. Cupertino, V. F. Mendes, H. A. Pereira, "Methodology for BESS Design Assisted by Choice Matrix Approach", *Eletrônica de Potência*, vol. 29, p. e202412, Jun. 2024, doi:10.18618/REP.2005.1.019027, URL: https://journal.sobraep.org.br/index.php/rep/article/view/916.

[7] K. Ribeiro, R. Santos, E. Saraiva, R. Rajagopal, "A Statistical Methodology to Estimate Soiling Losses on Photovoltaic Solar Plants", *Journal of Solar Energy Engineering*, vol. 143, no. 6, p. 064501, 05 2021, doi:10.1115/1.4050948.

[8] N. AL-Rousan, N. A. M. Isa, M. K. M. Desa, "Advances in solar photovoltaic tracking systems: A review", *Renewable and Sustainable Energy Reviews*, vol. 82, pp. 2548–2569, 2018, doi:https://doi.org/10.1016/j.rser.2017.09.077.

[9] A. Cabrera-Tobar, E. Bullich-Massagué, M. Aragüés-Peñalba, O. Gomis-Bellmunt, "Topologies for large scale photovoltaic power plants", *Renewable and Sustainable Energy Reviews*, vol. 59, pp. 309–319, 2016, doi:https://doi.org/10.1016/j.rser.2015.12.362, URL: https://www.sciencedirect.com/science/article/pii/S1364032116000289.

[10] M. Boyd, "NIST Weather Station for Photovoltaic and Building System Research", , 03 2016, doi:10.6028/NIST.TN.1913.

[11] S. Ansari, A. Ayob, M. S. H. Lipu, M. H. M. Saad, A. Hussain, "A Review of Monitoring Technologies for Solar PV Systems Using Data Processing Modules and Transmission Protocols: Progress, Challenges and Prospects", *Sustainability*, vol. 13, no. 15, 2021, doi:10.3390/su13158120.

[12] Q. Liu, Y. Zhao, Y. Zhang, D. Kang, Q. Lv, L. Shang, "Hierarchical context-aware anomaly diagnosis in large-scale PV systems using SCADA data", *in 2017 IEEE 15th International Conference on Industrial Informatics*, pp. 1025–1030, 2017, doi:10.1109/INDIN.2017.8104914.

[13] S. Baschel, E. Koubli, J. Roy, R. Gottschalg, "Impact of Component Reliability on Large Scale Photovoltaic Systems' Performance", *Energies*, vol. 11, no. 6, 2018, doi:10.3390/en11061579.

[14] U. Jahn, W. Nasse, "Operational performance of grid-connected PV systems on buildings in Germany", *Progress in Photovoltaics: Research and Applications*, vol. 12, no. 6, pp. 441–448, 2004, doi:https://doi.org/10.1002/pip.550.

[15] S. Gallardo-Saavedra, L. Hernández-Callejo, O. Duque-Perez, "Technological review of the instrumentation used in aerial thermographic inspection of photovoltaic plants", *Renewable and Sustainable Energy Reviews*, vol. 93, pp. 566–579, 2018, doi:https://doi.org/10.1016/j.rser.2018.05.027.

[16] M. Villarini, V. Cesarotti, L. Alfonsi, V. Introna, "Optimization of photovoltaic maintenance plan by means of a FMEA approach based on real data", *Energy Conversion and Management*, vol. 152, pp. 1–12, 2017, doi:https://doi.org/10.1016/j.enconman.2017.08.090.

[17] A. Betti, M. L. L. Trovato, F. S. Leonardi, G. Leotta, F. Ruffini, C. Lanzetta, "Predictive Maintenance in Photovoltaic Plants with a Big Data Approach", *CoRR*, vol. abs/1901.10855, 2019, 1901.10855.

[18] V. Smet, F. Forest, J.-J. Huselstein, F. Richardeau, Z. Khatir, S. Lefebvre, M. Berkani, "Ageing and Failure Modes of IGBT Modules in High-Temperature Power Cycling", *IEEE Transactions on Industrial Electronics*, vol. 58, no. 10, pp. 4931–4941, 2011, doi:10.1109/TIE.2011.2114313.

[19] M. Köntges, S. Kurtz, C. Packard, U. Jahn, K. Berger, K. Kato, T. Friesen, H. Liu, M. Van Iseghem, j. Wohlgemuth, D. Miller, M. Kempe, P. Hacke, F. Reil, N. Bogdanski, W. Herrmann, C. Buerhop, G. Razongles, G. Friesen, *Review of Failures of Photovoltaic Modules*, International Energy Agency, 2014, URL: https://iea-pvps.org/wp-content/uploads/2020/01/IEA-PVPS_T13-01_2014_Review_of_Failures_of_Photovoltaic_Modules_Final.pdf.

[20] Y. Wang, Q. Hu, L. Li, A. M. Foley, D. Srinivasan, "Approaches to wind power curve modeling: A review and discussion", *Renewable and Sustainable Energy Reviews*, vol. 116, p. 109422, 2019.

[21] P. Marti-Puig, J. Hernández, J. Solé-Casals, M. Serra-Serra, "Enhancing Reliability in Wind Turbine Power Curve Estimation", *Appl Sci*, vol. 14, p. 2479, 2024, doi:10.3390/app14062479.

[22] F. Bilendo, A. Meyer, H. Badihi, N. Lu, P. Cambron, B. Jiang, "Applications and Modeling Techniques of Wind Turbine Power Curve for Wind Farms—A Review", *Energies*, vol. 16, p. 180, 2023, doi:10.3390/en16010180, URL: https://www.mdpi.com/1996-1073/16/1/180.

[23] PVsyst SA, "PVsyst, commercial photovoltaic system simulation software", https://www.pvsyst.com/, [Accessed on 24 January 2024].

[24] The Solar Design Company, "PV*Sol, commercial photovoltaic system simulation software", https://pvsol.software/en/, [Accessed on 24 January 2024].

[25] International Electrotechnical Commission (IEC), *Photovoltaic System Performance – Part 1: Monitoring, Part 2: Capacity Evaluation Method, Part 3: Energy Evaluation Method*, IEC 61724-1:2021, IEC 61724-2:2017, IEC 61724-3:2017, 2021.

[26] P. A. Morettin, J. da Motta Singer, *Estatística e Ciência de Dados*, 1 ed., Editora LTC, São Paulo, 2022.

[27] R. H. French, L. S. Bruckman, D. Moser, S. Lindig, M. van Iseghem, B. Müller, J. S. Stein, M. Richter, M. Herz, W. V. Sark, F. Baumgartner, *Assessment of Performance Loss Rate of PV Power Systems*, International Energy Agency, Photovoltaic Power Systems Programme (IEA PVPS), 2021, URL: https://iea-pvps.org/wp-content/uploads/2021/04/IEA-PVPS-T13-22_2021-Assessment-of-Performance-Loss-Rate-of-PV-Power-Systems-report.pdf.

BIOGRAPHIES

Paulo Alberto Viana Vieira received his B.Sc. degree in electrical engineering from the Federal University of Itajubá, Brazil, in 2015, his M.Sc. degree in energy resources engineering from the Federal University of Itajubá, Brazil, in 2019, and his solar photovoltaic systems specialist certification from the Federal University of Viçosa, Brazil, in 2024. Since 2019, he has been working in O&M Manager for photovoltaic power plants, with more than 2.2 GWp of experience. His main research interests are renewable energy systems, solar photovoltaics, and energy storage systems.

João Marcus Soares Callegari received the B.Sc. degree in electrical engineering from the Federal University of Viçosa, Brazil, in 2019 and the M.Sc. degree in electrical engineering from the Federal Center of Technological Education of Minas Gerais, Brazil, in 2021. Currently, he is working toward the Ph.D. degree in electrical engineering at the Federal University of Minas Gerais, Brazil. His current research and technical interests include the design and control of grid-connected multifunctional inverters, the reliability of power electronics-based systems, and AC microgrids. Mr. Callegari was the recipient of the President Bernardes Silver Medal in 2019 and the IEEE IAS CMD Student Thesis Contest 2022 (Non-PhD Category).

Heverton Augusto Pereira received the B.S. degree in electrical engineering from the Federal University of Viçosa, Brazil, in 2007, the M.Sc. degree in electrical engineering from the University of Campinas, Brazil, in 2009, and the Ph.D. degree in electrical engineering from the Federal University of Minas Gerais, Brazil, in 2015. He was a visiting Researcher with the Department of Energy Technology, Aalborg University, Denmark, in 2014. In 2009, he joined the Department of Electrical Engineering, Federal University of Viçosa, where he is currently Professor. Since 2017 he has been a member of the pos-graduation program in Electrical Engineering from UFSJ/CEFET-MG and since 2020 he is Coordinator of Specialization in Photovoltaic System at Federal University of Viçosa. His research interests include grid-connected converters for photovoltaic systems and battery energy storage systems.